HHS Public Access

Author manuscript

Exp Neurol. Author manuscript; available in PMC 2023 December 01.

Published in final edited form as:

Exp Neurol. 2023 November ; 369: 114537. doi:10.1016/j.expneurol.2023.114537.

Epilepsy plus Blindness in Microdeletion of GABRA1 and GABRG2 in Mouse and Human

Qi Zhang, MD, PhD[1,2], **Cynthia Forster-Gibson, MD, PhD**[3], **Eduard Bercovici, MD**[4], **Alexandra Bernardo, PhD**[5], **Fei Ding, PhD**[2], **Wangzhen Shen, MD**[1], **Katherine Langer**[1], **Tonia Rex, PhD**[5], **Jing-Qiong Kang, MD, PhD**[1,6,7]

[1]Department of Neurology, Vanderbilt University Medical Center, Nashville, TN 37212

[2]Key Laboratory of Neuroregeneration of Jiangsu and Ministry of Education, Co-innovation Center of Neuroregeneration, Department of Neurology, Nantong University, 19 Qixiu Road, Nantong, JS 226001, PR China, Canada

[3]Laboratory Medicine and Genetics, Trillium Health Partners, Mississauga and Laboratory Medicine and Pathobiology, University of Toronto, Canada

[4]Division of Neurology, faculty of Medicine, University of Toronto, Canada

[5]Department of Ophthalmology & Visual Sciences Vanderbilt Eye Institute, Vanderbilt University Medical Center, Nashville, TN 37212

[6]Department of Pharmacology, Vanderbilt University; Nashville, TN 37212

[7]Vanderbilt Brain Institute and Vanderbilt Kennedy Center of Human Development, Vanderbilt University; Nashville, TN 37212

Abstract

Objective—$GABA_A$ receptor subunit gene (*GABR*) mutations are significant causes of epilepsy, including syndromic epilepsy. This report for the first time, describes intractable epilepsy and blindness due to optic atrophy in our patient, who has a microdeletion of the *GABRA1* and *GABRG2* genes. We then characterized the molecular phenotypes and determined patho-mechanisms underlying the genotype-phenotype correlations in a mouse model who is haploinsufficient for both genes ($Gabra1^{+/-}/Gabrg2^{+/-}$ mouse).

Methods—Electroencephalography was conducted in both human and mice with the same gene loss. $GABA_A$ receptor expression was evaluated by biochemical and imaging approaches. Optic nerve atrophy was evaluated with fundus photography in human while electronic microscopy, visual evoked potential and electroretinography recordings were conducted in mice.

Corresponding Author: Jing-Qiong Kang, M.D., Ph.D., Vanderbilt University Medical Center, 6140 Medical Research Building III, 465 21st Ave, South, Nashville, TN 37232-8552, Tel: 615-936-8399; fax: 615-322-5517, jingqiong.kang@vanderbilt.edu.

Author Contribution: QZ performed all biochemical, EEG recordings and electronic microscopy experiments. CFG and EB collected all the clinical data. AB Performed ERG experiment. FD support the study. KL edited the manuscript. JQK conceived the project, performed confocal microscopy, analyzed data. QZ and JQK wrote the manuscript. All authors edited the compiled manuscript.

Conflict of Interest statement: None of authors declared any conflict of interest.

We confirm that we have read the Journal's position on issues involved in ethical publication and affirm that this report is consistent with those guidelines

Results—The patient has bilateral optical nerve atrophy. Mice displayed spontaneous seizures, reduced electroretinography oscillatory potential and reduced $GABA_A$ receptor α1, β2 and γ2 subunit expression in various brain regions. Electronic microscopy showed that mice also had optic nerve degeneration, as indicated by increased G-ratio, the ratio of the inner axonal diameter to the total outer diameter, suggesting impaired myelination of axons. More importantly, we identified that phenobarbital was the most effective anticonvulsant in mice and the patient's seizures were also controlled with phenobarbital after failing multiple anti-seizure drugs.

Conclusions—This study is the first report of haploinsufficiency of two *GABR* epilepsy genes and visual impairment due to altered axonal myelination and resultant optic nerve atrophy. The study suggests the far-reaching impact of *GABR* mutations and the translational significance of animal models with the same etiology.

Keywords

$GABA_A$ receptors; epilepsy; blindness; copy number variation (CNV); optic nerve atrophy; Electroencephalography (EEG); Electroretinography (ERG)

INTRODUCTION

Genetic abnormalities in both *GABRA1 and GABRG2* have been associated with various epilepsy syndromes and with multiple comorbidities [1,2] (https://www.ncbi.nlm.nih.gov/clinvar/) (Figure 1A). The phenotype ranges from mild self-remitting childhood absence epilepsy (CAE) to much more severe seizure conditions such as Dravet syndrome and other typical or atypical epileptic encephalopathies.[3–5] The associated comorbidities are commonly reported as autism, anxiety, attention deficit hyperactivity disorder (ADHD) and impaired cognition, reflecting a broadly altered brain function. Single mutations have previously been reported in each of: *GABRA1, GABRA5, GABRB3, GABRB2* and *GABRG2*.[5–9] It might be expected that haploinsufficiency of more than one $GABA_A$ receptor (GABR) subunit gene might give rise to a more complicated phenotype than mutations in single genes. Some of the *GABR* genes are clustered together, for example, both *GABRA1 and GABRG2* genes are located at chromosome 5q34. Thus, a defect in a chromosome such as a continuous gene deletion may involve more than one *GABR* and give rise to a more complicated phenotype. Here, we report an individual with intractable epilepsy and functional blindness due to optic nerve atrophy, who has a copy number variation (CNV) (microdeletion) of both *GABRA1* and *GABRG2* at chromosome 5q34 resulting in haploinsufficiency. We characterized the equivalent condition in a mouse model with haploinsufficiency of both genes using multiple different methodologies.

METHODS

Next-generation sequencing

CGH array was 60K Oligo+SNP format using an Agilent 3 micron scanner and Cytosure platform.

Fundus photography

The camera used for fundus photography was a Canon CR-1 Digital Retinal Camera. The systems we used to capture the images were EOS 50D and Eyescape Advanced Imaging System.

Brain slice immunohistochemistry

All experimental procedures on mice were performed using protocols approved by Vanderbilt University Division of Animal Care. *Gabra1* and *Gabrg2* double knockout (*Gabra1*$^{+/-}$/*Gabrg2*$^{+/-}$, CNV) mouse line was generated by breeding *Gabra1*$^{+/-}$ with *Gabrg2*$^{+/-}$ in a C57BL/6J background. All mice used for the experiments were between 2-4 months old.

The brain sections were from freshly prepared brain tissues.[5] Mice were not perfused, and the brains were directly dissected and briefly fixed in 4% paraformaldehyde for 30 min and then maintained in a 30% sucrose solution before sectioning on a cryostat. The brains were sectioned at 15 to 30 μm. The sectioned tissues were stored at −20°C before staining. The brain slices were permeabilized with 0.4% triton for 10 min and blocked with 0.2%/0.2% BSA/Triton for 1 hr followed by immunoreaction overnight with specifically targeted antibodies. The slices were then gently washed with 0.1% BSA/PBA three times before incubating with secondary antibodies. The cell nuclei were labeled with TO-PRO-3 (Molecular Probes) with a 1:500 dilution for 1hr, washed and directly sealed with ProLong Gold antifade mounting medium (Molecular Probes).

Eye sample preparations and staining

Eye sample preparations and staining were based on our previous study.[10] Mice were decapitated and whole eyeballs directly dissected out and preserved in 4% PFA at room temperature overnight. Samples were then processed in 70% ethanol and paraffin embedded in a desired orientation and sectioned at 5 μm. Sectioned eye samples were mounted on Superfrost Plus slides for immunohistochemical studies. Slices were permeabilized with 0.1% triton for 10 min and blocked with 0.2% BSA for 1 hr followed by immunoreaction with specifically targeted antibodies overnight. The slices were then gently washed with 0.1%BSA/PBA three times before incubating with secondary antibodies. The slices were then processed with gradient alcohol (75%, 95%, and 100%) and rinsed with the hydrophobic clearing agent xylene for 2 min twice before being sealed with coverslips. The Hematoxylin and Eosin (HE) staining were performed with standard procedures in the Vanderbilt Translational Pathology Shared Resource Core.

Synchronized EEG recordings and analysis.

Synchronized video EEGs were recorded from 8 week to 4 month old C57BL/6J mice one week after electrode implantation and recorded with synchronized EEG monitoring system from Pinnacle Technology based on previous study.[11,12] Briefly, mice were anesthetized with 1–3% isoflurane and four epidural electrodes (stainless steel screws affixed to one head mount) were placed on the brain surface and secured in place with dental cement and surgical stiches. EMG leads were inserted into the trapezius muscle. Mice were allowed to recover from the EEG head mount implantation surgery for one week before EEG recording.

Video-EEG monitoring lasted for 24-48 hrs, and mice were freely moving during EEG recordings. Mouse behaviors such as behavioral arrest, myoclonic jerks or generalized tonic clonic seizures during the EEG recordings were identified to determine if mice exhibit behavioral seizures. At least 24 hours of baseline EEG recordings were obtained and analyzed for each mouse. The experimental details for drug treatment were included in Supplementary material.

Visual evoked potential (VEP) and Electroretinography (ERG) recordings

Mice were dark-adapted overnight, dilated with tropicamide for 10 min, and anesthetized with 20 mg/kg ketamine/ 8 mg/kg xylazine/ 8 mg/kg urethane. Mice were placed on the heated surface of the ERG system to maintain body temperature. Flash ERG was recorded from both eyes using a Celeris system (Diagnosys LLC, Cambridge, UK). The recording procedures were followed as previously described.[13] Briefly, 2-4 months old mice were dark-adapted overnight and then anesthetized with ketamine/xylazine (25/8 mg/kg body weight). 1% tropicamide solution was administered to the eyes for pupil dilatation and the mice were placed on a heated mouse platform (Lowell, MA). Mice were exposed to flashes of light in a dark room with only a dim red light on. The amplitude of a_{max} was measured from baseline to peak and the amplitude of the b_{max} was measured from trough to peak after exposure to a 1.0 log cd*s/m^2 flash of light. Recordings from a minimum of 5 mice of each genotype were analyzed.

Optic nerve preparation and electron microscopy (EM)

Sample preparations of optic nerves for electron microscopy were based on previous study.[14] The mice were not perfused and the optic nerves were directly fixed in pre-cooled 2.5% glutaraldehyde for at least 24 h, then post-fixed with 1% osmium tetraoxide solution, dehydrated stepwise in increasing concentrations of ethanol, and embedded in Epon 812 epoxy resin. Ultrathin sections dissected at 70 nm were stained with lead citrate and uranyl acetate, and then pictures were taken under a transmission electron microscope (JEOL Ltd., Tokyo, Japan). The optic nerves were taken from 3 mice, 2-4 months old, for each group.

Statistical analysis

Protein integrated density values (IDVs) were quantified by using the Quantity One or Odessy fluorescence imaging system (Li-Cor). Data were expressed as mean ± SEM values and analyzed with GraphPad Prism 5.0 software. Statistical significance was determined by a Student’s unpaired t test, One-way or two-way ANOVA test with post hoc test for multiple comparisons. All analyses used an alpha level of 0.05 to determine statistical significance. Data were presented as Mean ± SEM.

RESULTS

Patient history

A 44-year-old man began to have febrile seizures at 9 months of age and later developed afebrile seizures, including generalized tonic clonic seizures (GTCS) that decreased in frequency with age. As a teen, he began to have “petit mal” seizures and in adulthood he developed complex partial seizures. At age 32, he had occipital seizures,

refractory to medication and ketogenic diet. He continues to have monthly seizures on Cannabidiol, Divalproex and Fycompa. Multiple EEGs show multifocal independent spikes, predominantly in the left quandrant. Optic atrophy was noted at 4 years of age, and he is now legally blind.

Microarray

Both *GABRA1* and *GABRG2* are established epilepsy genes that have been associated with various epilepsy syndromes (Figure 1A). Microarray analysis identified a likely pathogenic copy number variant (CNV). This was a loss of 2.22 Mb in chromosome region 5q34 (161,217,464-163,441,003x1) (hg 19) resulting in heterozygous loss of *GABRA1* and *GABRG2* (Figure 1B) while the other $GABA_A$ receptor subunit *GABRB2* in the same chromosome was not included in the deletion. No other family members have had seizures or vision loss.

Visual impairment and fundus photography

By the age of 4 years, he was noted to have very poor vision and optic atrophy, and he was enrolled in the Canadian National Institute for the Blind. Bilateral optic nerve atrophy is shown by the pale color of optic papillae, indicating optic nerve atrophy (Figure 1C). His visual acuity is currently 20/800 (OD, right eye) and 20/1000 (OS, left eye) and he requires optical aids such as magnifiers, closed-circuit TV and voice over text (Figure 1D).

Eye phenotypes with electrophysiological and electronic microscopic evaluations in mice with CNV of GABRA1 and GABRG2.

We modeled the patient condition by generating *Gabra1*$^{+/-}$/*Gabrg2*$^{+/-}$ double knockout (*CNV*) mice in C57BL/6J background (*CNV* mouse). The *CNV* mice at 2-4 months of age had abnormal VEP (Figure 2A). Increased amplitude in VEP in the *CNV* mice may suggest a compensatory evoked potential with loss of function of *Gabra1* and *Gabrg2* but this needs to be further elucidated. Hematoxylin and Eosin (HE) staining of retinal sections showed no significant change of retinal gross lamination and cellular structure (Figure 2B). Electron microscopy analysis of optic nerves was performed to measure the layers of myelin and g-ratio of each genotype (Figure 2C–E). The data showed that, in *CNV* mice, myelin lamellae of the optic nerve decreased, while g-ratio increased, indicating an optic nerve degeneration. There was no change in the *Gabra1*$^{+/-}$ or *Gabrg2*$^{+/-}$ mouse.

Brain phenotypes with molecular and EEG evaluations.

The western blot data showed that total α1 and γ2 subunit proteins were reduced in all major brain regions including cortex, cerebellum, hippocampus and thalamus in *CNV* mice. The total β2 subunit protein was also reduced in *CNV* mice except in cerebellum (Figure 3A–E). Fluorescent immunostaining confirmed the decrease of α1 subunit (red) and γ2 subunit (green) expression as reduced total fluorescence intensity of α1 subunit (48.2±7.9 for wildtype vs 26.6±4.1, N=6, P<0.0356) or γ2 subunit (41.0±5.7 for wildtype vs 19.3±3.1, N=6, p=0.0074) in cortex of *CNV* mice (Figure 3F). Reduced expression of α1 subunit or γ2 subunit was also observed in various brain regions in the *Gabra1*$^{+/-}$ or *Gabrg2*$^{+/-}$ mouse but to less extent than the CNV mouse.

We then evaluated the seizure activity in the *CNV* mice by video monitoring synchronized EEG recordings at baseline and with pentylenetetrazol (PTZ, 30mg/kg) challenge (Figure 4A). Our previous studies have reported increased brief spike wave discharges (SWDs) in *Gabra1*$^{+/-}$ mice and *Gabrg2*$^{+/-}$ mice.[1,9,11,15,16] However, the *CNV* mice had more prolonged ictal discharges compared with both *Gabra1*$^{+/-}$ mice and *Gabrg2*$^{+/-}$ mice (data not shown). Additionally, *CNV* mice had occurrence of spontaneous generalized tonic-clonic seizures (GTCS) (Figure 4B), which is absent from *Gabra1*$^{+/-}$ or *Gabrg2*$^{+/-}$ mice. Both seizure severity and mortality were attenuated by phenobarbital (PB, 50mg/kg) at either baseline (Figure 4C) recordings or as challenged by PTZ (50mg/kg), We have tested other antiseizure drugs such as diazepam (DZP, 0.3mg/kg), cannabidiol (CBD, 10mg/kg) and vigabatrin (VGB, 100mg/kg). We tried a higher dose of CBD (20mg/kg) but the mice appeared to be very agitated, so we thus used 10mg/kg instead. Interestingly, PB was the most effective among all the tested antiseizure drugs. ***(A special note: the patient was switched to PB 100mg per day after this finding and his seizures were well controlled***).

DISCUSSION

Previous studies have reported various mutations in *GABR* which give rise to a wide spectrum of clinical phenotypes of epilepsy. The phenotype for GABR*A1* mutations includes childhood absence epilepsy (CAE), juvenile myoclonic epilepsy and Dravet syndrome while the phenotype for *GABRG2* mutations include febrile seizures, CAE, Dravet syndrome and various atypical epileptic encephalopathy.[9,17,18] This study describes novel genotypic, clinical, and molecular presentations of haploinsufficiency (CNV) of *GABRA1 and GABRG2*. The study thus expands the spectrum of $GABA_A$ receptor gene variants and clinical phenotypes and further supports the heterogeneity of epilepsy and its associated comorbidities.

This is the first report of blindness and optic atrophy in an individual with epilepsy due to *GABR CNV*. However, the role of $GABA_A$ circuits is established in visual cortical plasticity[19,20]. It has also been observed the white matter alterations in epilepsy[21,22]. The phenotype was recapitulated by a mouse model with loss of both *GABRA*1 and *GABRG2 (Gabra1*$^{+/-}$*/Gabrg2*$^{+/-}$, CNV). Although there was no obvious abnormality in retinal lamination, the *CNV* mice had upregulated VEP that may suggest an unknown compensatory increase of evoked potential in the mutant mice but this merits further investigation. There was reduced amplitude in the oscillatory potentials as well as A-wave maximum (a_{max}) and B-wave maximum (b_{max}) in ERG (data not shown). EM indicated degeneration or malformation of the optic nerve in *CNV* mice as myelin lamellae of the optic nerve were decreased and the g-ratio increased. We had previously identified that *Gabrb3*$^{+/-}$ knockout mice, representing Angelman syndrome[23], have reduced ocular pigmentation[10]. Light eye color is common in Angelman syndrome caused by microdeletion. Additionally, mutations in *GABRG2* alone have been associated with epileptic encephalopathy and eye movement disorder such as roving eye movements[9], suggesting that a defective GABAergic pathway may alter visual function. This is not surprising given the abundant presence of $GABA_A$ receptors in retina.[24] The anti-seizure drug VGB, an irreversible inhibitor of GABA transaminase has retinal toxicity and causes vision loss. Together, this indicates that the function of $GABA_A$ receptor is critical for eye

development whereas dysfunction of $GABA_A$ receptors could result in variable brain and visual disorders.

It is worth noting that mutations in *GABRG2* alone have been associated with epileptic encephalopathy, white matter atrophy and delayed myelination as reflected by falx hypoplasia or volume loss. White matter abnormality is common in epilepsy[25] During early brain development, oligodendrocyte progenitor cells are paired with GABA neurons, suggesting that GABA signaling is critical for myelination.[26] On the other hand, blocking synaptic vesicle release impairs CNS myelination.[27] Although this study didn't characterize the brain white matter at either the structural or molecular level, it is plausible that impaired GABA signaling during early brain development due to mutations in *GABRs* could affect oligodendrocytes or other cell maturation and function. The altered axonal myelination of optic nerve in both human and mouse with haploinsufficiency of *GABRA1* and *GABRG2* indicates poor myelination in at least some epileptic brains, but this merits further investigation.

We have substantially characterized mutations in both *GABRA1* and *GABRG2* in cell and mouse models. Our findings indicate that these mutations can give rise to variable epilepsy phenotypes based on the nature of the mutation[28] and possibly the patient's genetic background. The seizure phenotype in the individual reported here evolved from febrile seizures to GTCS, "petite mal", complex partial and occipital seizures, refractory to multiple AEDs. Phenobarbital was tried briefly at an early age but was stopped due to side effects. We evaluated multiple AEDs in *CNV* mice, finding that phenobarbital was relatively efficacious in reducing seizures. We then informed the patient's physician about the finding in mice and were told that the patient became seizure free after being switched to phenobarbital.

In conclusion, the study extends the molecular genetics and clinical phenotypes for two known epilepsy genes *GABRA1* and *GABRG2* and reports an unusual comorbidity, blindness due to optic nerve atrophy, in an individual with epilepsy due to *GABRA1 and GABRG2* haploinsufficiency. The study identified the most effective treatment in suppressing seizures and reducing mortality in the mouse model with CNV of the same gene. It is not known if this is relevant for clinical anticonvulsant selection for patients with $GABA_A$ receptor deficiency. The study suggests that attention should be paid to visual impairment and white matter alterations in epilepsy patients with *GABR* mutations. This study also implies that impaired $GABA_A$ receptor function may alter white matter integrity but needs further in-depth study.

Supplementary Material

Refer to Web version on PubMed Central for supplementary material.

Acknowledgements:

Research was supported by grants from Citizen United for Research in Epilepsy (CURE), Dravet syndrome foundation (DSF), Vanderbilt Brain Institute Award and Vanderbilt Clinical and Translation Science Award and NINDS R01 NS082635, NS1211718. Natural Science Foundation of Jiangsu Province No BK20161285. DoD W81XWH-15-1-0096, W81XWH-17-2-0055; NIH NEI R01EY022349, U24EY029893; Ayers Research Fund in

Regenerative Visual Neuroscience; Potocsnak Family-CSC Research Fund; Ret. Maj. General Stephen L. Jones, MD Fund; Research to Prevent Blindness Unrestricted Funds (VEI); NIH P30 EY008126 (VVRC). Imaging data were performed in part through the VUMC Cell Imaging Shared Resource. Special thanks to Zhu Li and Marco Dong for their excellent technical assistance.

REFERENCES

1. Kang JQ & Macdonald RL Molecular Pathogenic Basis for GABRG2 Mutations Associated With a Spectrum of Epilepsy Syndromes, From Generalized Absence Epilepsy to Dravet Syndrome. JAMA neurology 73, 1009–1016 (2016). 10.1001/jamaneurol.2016.0449 [PubMed: 27367160]
2. Macdonald RL, Kang JQ & Gallagher MJ in Jasper's Basic Mechanisms of the Epilepsies (eds th et al.) (2012).
3. Mefford HC et al. Rare copy number variants are an important cause of epileptic encephalopathies. Annals of neurology 70, 974–985 (2011). 10.1002/ana.22645 [PubMed: 22190369]
4. Wallace RH et al. Mutant GABA(A) receptor gamma2-subunit in childhood absence epilepsy and febrile seizures. Nature genetics 28, 49–52 (2001). 10.1038/88259 [PubMed: 11326275]
5. Kang JQ, Shen W, Zhou C, Xu D & Macdonald RL The human epilepsy mutation GABRG2(Q390X) causes chronic subunit accumulation and neurodegeneration. Nat Neurosci 18, 988–996 (2015). 10.1038/nn.4024 [PubMed: 26005849]
6. Ishii A et al. A de novo missense mutation of GABRB2 causes early myoclonic encephalopathy. J Med Genet 54, 202–211 (2017). 10.1136/jmedgenet-2016-104083 [PubMed: 27789573]
7. Hernandez CC et al. Altered inhibitory synapses in de novo GABRA5 and GABRA1 mutations associated with early onset epileptic encephalopathies. Brain : a journal of neurology 142, 1938–1954 (2019). 10.1093/brain/awz123 [PubMed: 31056671]
8. Shi YW et al. Synaptic clustering differences due to different GABRB3 mutations cause variable epilepsy syndromes. Brain 142, 3028–3044 (2019). 10.1093/brain/awz250 [PubMed: 31435640]
9. Shen D et al. De novo GABRG2 mutations associated with epileptic encephalopathies. Brain : a journal of neurology 140, 49–67 (2017). 10.1093/brain/aww272 [PubMed: 27864268]
10. Delahanty RJ et al. Beyond Epilepsy and Autism: Disruption of GABRB3 Causes Ocular Hypopigmentation. Cell reports 17, 3115–3124 (2016). 10.1016/j.celrep.2016.11.067 [PubMed: 28009282]
11. Warner TA et al. Differential molecular and behavioural alterations in mouse models of GABRG2 haploinsufficiency versus dominant negative mutations associated with human epilepsy. Human molecular genetics 25, 3192–3207 (2016). 10.1093/hmg/ddw168 [PubMed: 27340224]
12. Warner TA, Liu Z, Macdonald RL & Kang JQ Heat induced temperature dysregulation and seizures in Dravet Syndrome/GEFS+ Gabrg2(+/Q390X) mice. Epilepsy research 134, 1–8 (2017). 10.1016/j.eplepsyres.2017.04.020 [PubMed: 28505490]
13. Bernardo-Colon A et al. Antioxidants prevent inflammation and preserve the optic projection and visual function in experimental neurotrauma. Cell death & disease 9, 1097 (2018). 10.1038/s41419-018-1061-4 [PubMed: 30367086]
14. Gu Y et al. Chitosan/silk fibroin-based, Schwann cell-derived extracellular matrix-modified scaffolds for bridging rat sciatic nerve gaps. Biomaterials 35, 2253–2263 (2014). 10.1016/j.biomaterials.2013.11.087 [PubMed: 24360577]
15. Arain FM, Boyd KL & Gallagher MJ Decreased viability and absence-like epilepsy in mice lacking or deficient in the GABAA receptor alpha1 subunit. Epilepsia 53, e161–165 (2012). 10.1111/j.1528-1167.2012.03596.x [PubMed: 22812724]
16. Zhang CQ et al. Molecular basis for and chemogenetic modulation of comorbidities in GABRG2-deficient epilepsies. Epilepsia 60, 1137–1149 (2019). 10.1111/epi.15160 [PubMed: 31087664]
17. Harkin LA et al. Truncation of the GABA(A)-receptor gamma2 subunit in a family with generalized epilepsy with febrile seizures plus. Am J Hum Genet 70, 530–536 (2002). 10.1086/338710 [PubMed: 11748509]
18. Carvill GL et al. GABRA1 and STXBP1: novel genetic causes of Dravet syndrome. Neurology 82, 1245–1253 (2014). 10.1212/WNL.0000000000000291 [PubMed: 24623842]

19. Fagiolini M et al. Specific GABAA circuits for visual cortical plasticity. Science 303, 1681–1683 (2004). 10.1126/science.1091032 [PubMed: 15017002]
20. Hensch TK Critical period plasticity in local cortical circuits. Nat Rev Neurosci 6, 877–888 (2005). 10.1038/nrn1787 [PubMed: 16261181]
21. de Curtis M, Garbelli R & Uva L A hypothesis for the role of axon demyelination in seizure generation. Epilepsia 62, 583–595 (2021). 10.1111/epi.16824 [PubMed: 33493363]
22. Deleo F et al. Histological and MRI markers of white matter damage in focal epilepsy. Epilepsy Res 140, 29–38 (2018). 10.1016/j.eplepsyres.2017.11.010 [PubMed: 29227798]
23. DeLorey TM et al. Mice lacking the beta3 subunit of the GABAA receptor have the epilepsy phenotype and many of the behavioral characteristics of Angelman syndrome. The Journal of neuroscience : the official journal of the Society for Neuroscience 18, 8505–8514 (1998). [PubMed: 9763493]
24. Cai YQ et al. Mice with genetically altered GABA transporter subtype I (GAT1) expression show altered behavioral responses to ethanol. Journal of neuroscience research 84, 255–267 (2006). 10.1002/jnr.20884 [PubMed: 16683252]
25. Focke NK et al. Idiopathic-generalized epilepsy shows profound white matter diffusion-tensor imaging alterations. Human brain mapping 35, 3332–3342 (2014). [PubMed: 25050427]
26. Boulanger JJ & Messier C Oligodendrocyte progenitor cells are paired with GABA neurons in the mouse dorsal cortex: Unbiased stereological analysis. Neuroscience 362, 127–140 (2017). 10.1016/j.neuroscience.2017.08.018 [PubMed: 28827179]
27. Mensch S et al. Synaptic vesicle release regulates myelin sheath number of individual oligodendrocytes in vivo. Nature neuroscience 18, 628–630 (2015). 10.1038/nn.3991 [PubMed: 25849985]
28. Kang JQ, Shen W & Macdonald RL Trafficking-deficient mutant GABRG2 subunit amount may modify epilepsy phenotype. Annals of neurology 74, 547–559 (2013). 10.1002/ana.23947 [PubMed: 23720301]

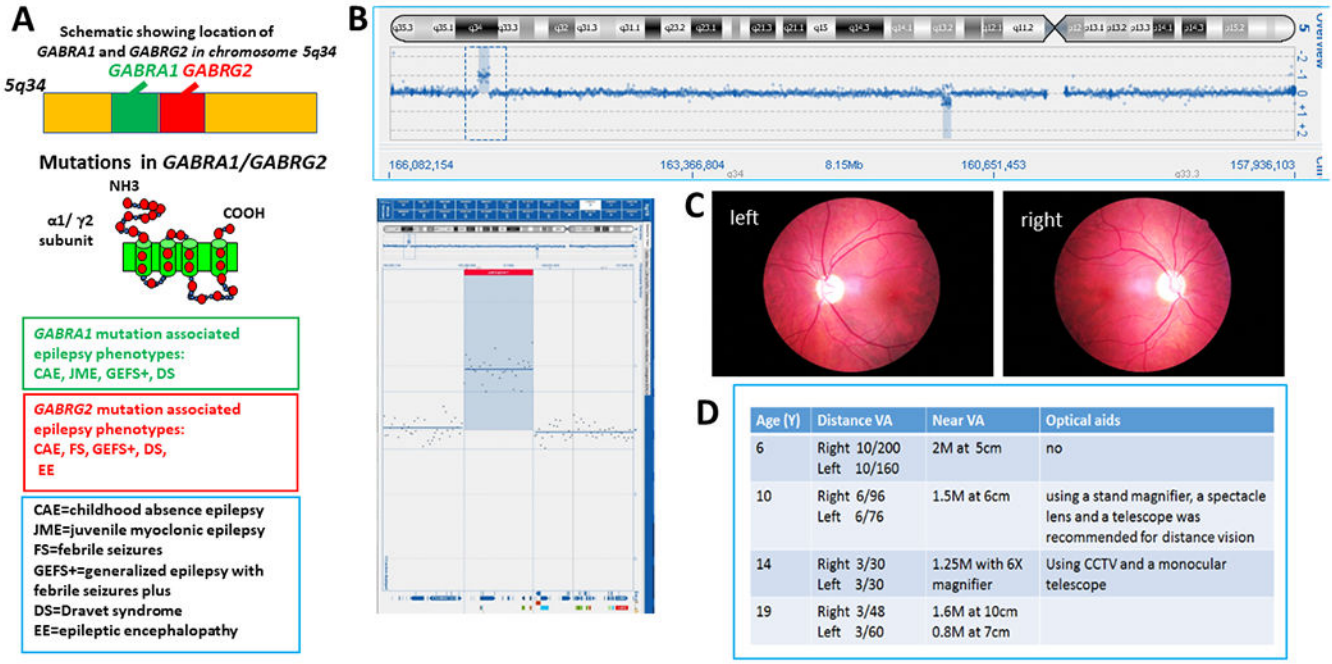

Figure 1. Molecular genetics and clinical phenotype in a patient with copy number variation (CNV) of GABRA1 and GABRG2 due to a microdeletion in chromosome 5q34.

(A) Schematic showing the adjacency of *GABRA1* and *GABRG2* in chromosome 5q34 (top panel). Over 200 variations/mutations in either *GABRA1* or *GABRG2* have been associated with various epilepsy syndromes. These mutations are distributed in various locations and domains of the α1 or γ2 subunit. The red dots represent the relative locations of the epilepsy-related mutations (middle panel). Mutation in either *GABRA1* or *GABRG2* are associated with variable seizure disorders or epilepsy syndromes (lower panel). **(B)** Microarray showing reduced copy numbers of *GABRA1* and *GABRG2* in chromosome 5q34. **(C)** Fundus photography showing pale color of optic papillae for both eyes**. (D)** Vision assessment showing reduced vision acuity of patient at different ages.

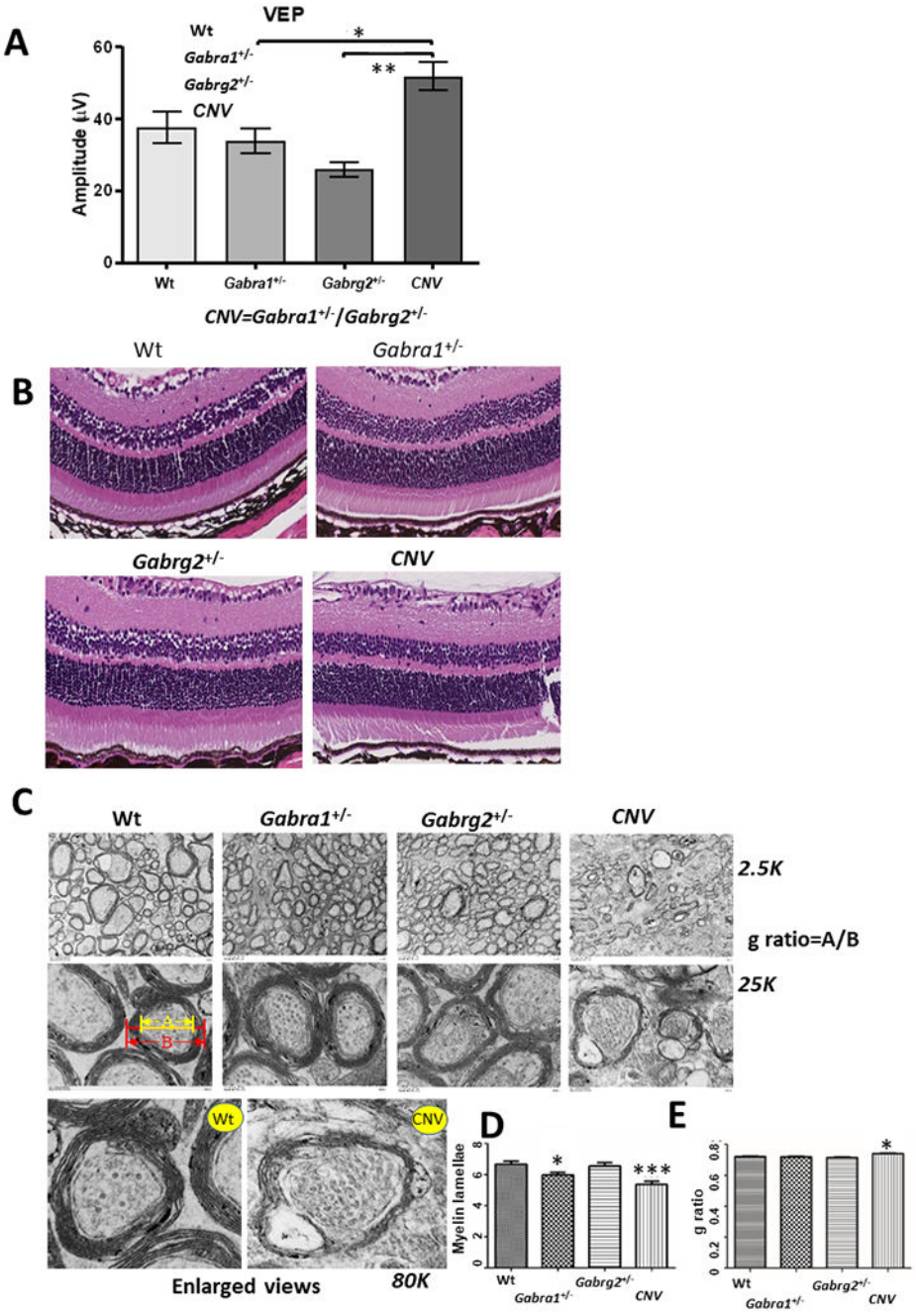

Figure 2. Electroretinaography (ERG) and electronic microscopy (EM) evaluation of optic nerves in mice with CNV of GABRA1 and GABRG2.

(A) Flash Electroretinography (ERG) was recorded from both eyes of 2-4 month-old mice using a Celeris system. Briefly, mice were dark-adapted overnight and then exposed to flashes of light in a dark room with only a dim red light on. The amplitude of visual evoked potential (VEP) was measured (N=9 for all genotypes except 5 for deletion of both *Gabra1* and *Gabrg2* (*Gabra1*$^{+/-}$/*Gabrg2*$^{+/-}$, *CNV*). *P<0.05 vs *Gabra1*$^{+/-}$, **P<0.01 vs *Gabrg2*$^{+/-}$. **(B)** Eye samples from 2-4 month-old mice of the wildtype, *Gabra1*$^{+/-}$, *Gabrg2*$^{+/-}$ and *CNV*

groups were fixed in 4% paraformaldehyde (wt/vol) overnight and then paraffin embedded in the desired orientation and sectioned at 5 μm. Hematoxylin and Eosin (HE) staining of retinal sections was performed. **(C)** The optic nerve was taken from 3 mice, of 2-4 months old, for each group, fixed with pre-cooled 2.5% glutaraldehyde, post-fixed with 1% osmium tetraoxide solution, dehydrated stepwise in increasing concentrations of ethanol, and embedded in Epon 812 epoxy resin. The samples were dissected at 70 nm and stained with lead citrate and uranyl acetate. Representative images from transmission electron microscopy (TEM) showed the cross-section of optic nerves. **(D)** The layers of myelin lamellae of each phenotype were counted (n=95 for Wt, n=106 for *Gabra1*$^{+/-}$, n=83 for *Gabrg2*$^{+/-}$, n=85 for *CNV*, one-way ANOVA and Tukey's multiple comparisons. P= 0.0485 vs Wt for *Gabra1*$^{+/-}$, P < 0.0001 vs Wt for *CNV*. Error bars represent SE.). **(E)** G-ratio is defined as the ratio of the inner axonal diameter (A) to the total outer diameter (B), which is widely utilized as a functional and structural index of optimal axonal myelination. (n=300 for Wt, n=392 for *Gabra1*$^{+/-}$, n=427 for *Gabrg2*$^{+/-}$, n=231 for *CNV*, one-way ANOVA and Tukey's multiple comparisons. P= 0.0141vs Wt). In **D** and **E**, *P<0.05, ***P<0.001 vs Wt.

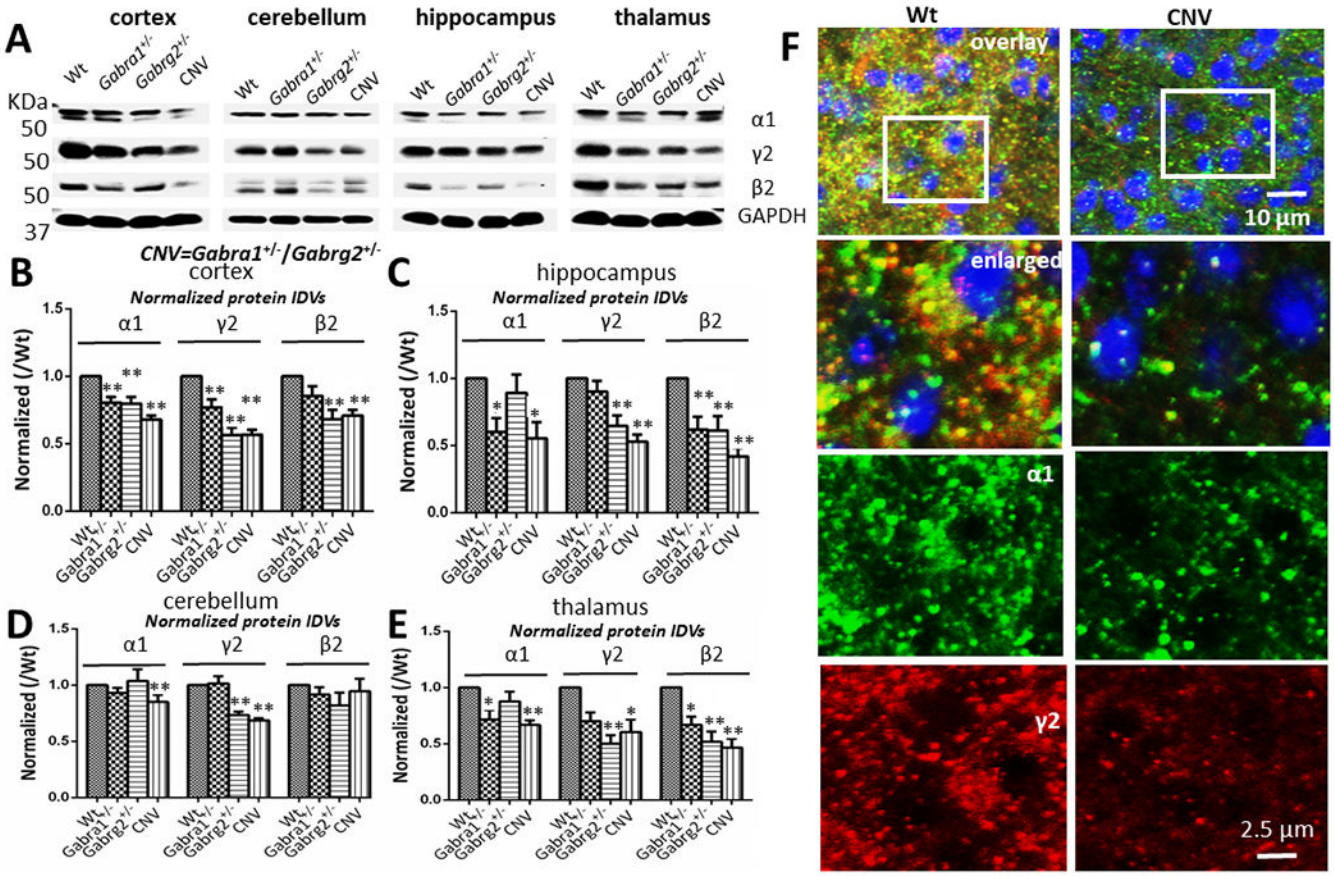

Figure 3. Biochemical and histochemical characterizations of brain of mice with CNV of GABRA1 and GABRG2 indicated reduction of other partnering subunits in addition to α1 and γ2 subunits

(A) Total lysates of different brain regions (cortex, cerebellum, hippocampus and thalamus) from mice at ages 2-4 months were analyzed by western blot and immunoblotted with a mouse monoclonal anti-α1 subunit antibody, a rabbit polyclonal anti-β2 or anti-γ2 subunit antibodies. (**B-E)** Graphs showing protein IDVs in the mutant mice normalized to the wildtype which was arbitrarily taken as 1. Each specific protein was normalized to its internal control GAPDH first and then to wildtype (one-way ANOVA and Tukey's multiple comparisons. Error bars represent SE). **(F)** Representative images from fluorescent immunostaining of the brain slices sectioned at 30 μm showed the reduced expressions of α1 subunit (red) and γ2 subunit (green) in the cortex of CNV mice. In **B**, **C**, **D** and **E**, *P<0.05, **P<0.01, vs Wt.

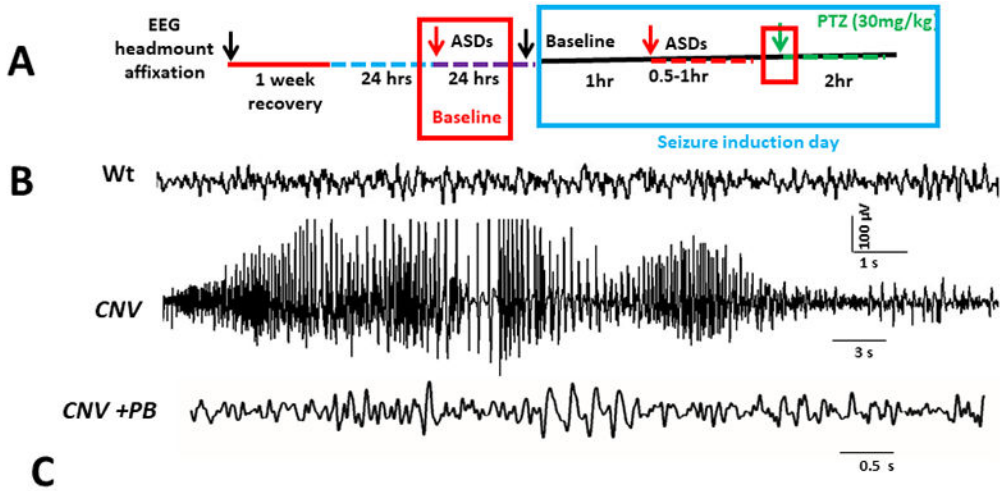

C

Group	Animal No	Female vs male	GTCS No	SWDs frequency	SWDs duration	Mortality After PTZ	dosage (mg/kg)
Wt	26	12,14	0	2.1	1.21	0	
CNV	14	7, 7	2.54	§§ 25.6	§ *** 2.42	** 4/14	
CNV+DZP	11	5,6	1.82	21.2	1.97	2/11	0.3
CNV+CBD	8	4,4	2.25	18.6	1.85	1/8	10
CNV+VGB	9	5,4	1.6	26.8	2.04	1/9	100
CNV+PB	12	6, 6	0	5.7	1.45	0	50
			Baseline			challenged	

Figure 4. Electrophysiological characterizations of mice with CNV of GABRA1 and GABRG2 and identification of an effective antiseizure drug.

(A) A diagram of baseline EEG recordings and seizure induction procedure with pentylenetetrazol (PTZ, 30mg/kg, intraperitoneal injection, IP) is shown. Normally, mice underwent 1 week recovery after EEG headmount affixation surgery. Each mouse had at least 24 hrs of baseline EEG recordings and then treated with different anti-seizure drugs (ASDs) followed by another 24 hr recordings (baseline). Seizure induction test immediately followed the 24 hr baseline recording. On the day of seizure induction test, each mouse had an additional 1 hr baseline recording before administration of antiseizure drugs (ASDs) to ensure the recording was stable. Antiseizure drugs (AEDs) were administered 30 min or 1hr ((30min for Diazepam, DZP (0.3mg/kg) or 1hr (for Cannabidiol, CBD (10 mg/kg); Vigabatrin, VGB (100mg/kg) and phenobarbital, PB(50mg/kg)) before seizure induction with pentylenetetrazol (PTZ, 30mg/kg). **(B)** Mice, 2-4 months old, of the wildtype, *Gabra1*$^{+/-}$, *Gabrg2*$^{+/-}$ and *CNV* groups were implanted with prefabricated skull head mounts and after at least 1 week of recovery, 24 h synchronized video-EEG/EMG recordings were obtained. **(C)** The effect of phenobarbital on suppressing seizure activity at baseline recordings (24 hrs) or reducing mortality during PTZ (50mg/kg, IP) seizure induction was evaluated. The total number of seizures during 24 hrs baseline recordings was reported (C). During PTZ treatment, only mortality was reported because there was loss of some mice during the test. In **C**, **P<0.01, ***P<0.001 vs wt.; §P<0.05, §§P<0.01 vs CNV+PB.